Analysis of the Eddy Dissipation Concept formulation for MILD combustion modeling

Michał T. Lewandowski[a,*], Ivar S. Ertesvåg[b]

[a] *Institute of Fluid Flow Machinery, Polish Academy of Sciences, Gdańsk, Poland*
[b] *Department of Energy and Process Engineering, NTNU Norwegian University of Science and Technology, Trondheim, Norway*

Abstract

Performance of the Eddy Dissipation Concept (EDC) in the regime of Moderate and Intense Low-oxygen Dilution (MILD) combustion is investigated. The special MILD features, where chemical and turbulence time scales are comparable (Damköhler number close to unity), have led several researchers to suggest modifications of EDC, mainly by changing model constants. EDC with standard and modified constants are compared, and the importance of each effect is outlined. Different fine-structure reactor models and their inflow/initial conditions are discussed and found to play a significant role. The reacting fraction of fine structures, which in virtually all other numerical studies is set to unity, is also discussed and found to be important. We observe better agreement with experiment when the reacting fraction is reduced below unity, which is also described by the original EDC. The results obtained with the variable reacting fraction are found to improve both the temperature distributions and the lift-off height predictions. The calculations are carried out with the use of open source software OpenFOAM. The main test case was the Delft Jet-in-Hot-Coflow burner emulating MILD regime at three different flow conditions (jet Reynolds numbers of 2500, 4100 and 8800).

Keywords: MILD combustion, Eddy Dissipation Concept, Jet-in-Hot-Coflow, modelling, reacting fraction

1. Introduction

Moderate and Intense Low-oxygen Dilution (MILD) combustion is a modern and promising technique for increasing thermal efficiency and decreasing pollutant emissions in combustion systems. The technique is also called Flameless Oxidation (FLOX) [1], Highly Preheated Air Combustion (HPCA) [2], or High Temperature Air Combustion (HiTAC). Four decades ago it was known as Excess Enthalpy Combustion (EEC) [3]. The requirements for MILD combustion are that the inlet temperature of reactants is higher than the auto-ignition temperature of the mixture and that the temperature increase due to combustion is limited [4]. This method of combustion is also characterized by hardly visible flame, inherent flame stabilization, slow reaction rate, nearly-uniform temperature fields and smooth radiation flux, which is required in some industrial processes. Fundamental aspects of MILD combustion of different types of fuels were presented by Weber et al. [5], with a focus on industrial applications. Some issues of its mathematical modeling were raised by Mancini et al. [6].

The most common configuration that leads to MILD combustion is strong recirculation of exhaust gases into the fresh air, to heat it and to reduce the oxygen concentration. In laboratory scale flames, this can be achieved with Jet-in-Hot-Coflow burners [7, 8]. Furthermore, cases where both reactants are preheated are getting more common as well [9]. Most of the numerical and experimental studies concern fuels containing mainly methane, however, it is worth

*Corresponding author
Email addresses: michal.lewandowski@imp.gda.pl (Michał T. Lewandowski), ivar.s.ertesvag@ntnu.no (Ivar S. Ertesvåg)

pointing out that MILD combustion obtained with so-called Hot Diluted Fuel [10] configuration is very attractive for the combustion of low-calorific-value gases derived from gasification processes [9].

The Eddy Dissipation Concept (EDC) for turbulent combustion by B.F. Magnussen and co-workers [11, 12, 13, 14, 15] is a chemistry-turbulence interaction model, which represents a turbulent mixing approach. This kind of model seems to be a natural choice for MILD combustion modeling since mixing processes, together with finite rate chemistry, are more important in MILD than in conventional diffusion flames. The Damköhler number is usually low and often approaches unity in the MILD conditions, as the chemistry and mixing time scales are comparable. Other popular methods have also been used in this field, with greater or lesser success. The standard flamelet approach conceptually fails in the MILD regime as the smallest turbulence scales strongly affect the reaction zones. Therefore, no laminar flame structures may by identified [16]. The use of the standard flamelet approach, involving scalar gradient related quantities, was questioned by Minamoto et al. [17]. It was also investigated and confirmed by, for instance, Christo and Dally [18], Parente et al. [19, 20] and Rebola et al. [21] that this approach did not perform well in the MILD combustion regime. However, Ihme et al. [22] obtained good results when doing simulations of jet-in-hot-coflow flames with the use of a three-stream flamelet/progress variable (FPV) formulation in Large Eddy Simulations (LES). To account for ternary mixing, Locci et al. [23] proposed a new LES model based on diluted homogeneous reactors, and recently, Colin and Michel [24] presented a two-dimensional tabulated flamelet combustion model for furnace applications in the Reynolds Averaged Navier-Stokes (RANS) simulations. They applied the models to the flameless burner of Verissimo et al. [25], on which they reported under-prediction of the temperature at some locations. The Flamelet Generated Manifold (FGM) method is also under the development to capture MILD combustion features [26]. Worth mentioning is the transported-PDF method, which however was reported to be sensitive to the level of velocity fluctuations and has a higher computational cost [20, 27, 28], at least in the RANS turbulence approach. The Conditional Moment Closure (CMC) method was investigated e.g. by Kim et al. [29] as an alternative choice for MILD combustion modeling and by Tyliszczak [30] in the simulations of autoignitive hydrogen jet flames issuing into a hot ambient co-flow. Recently, akin method was adopted by Labahn et al. [31, 32], who developed Conditional Source-term Estimation (CSE) accounting for two mixture fraction both for RANS [31] and LES [32] tested on the Delft-Jet-in-Hot-Coflow (DJHC) flames [7].

In the engineering application, EDC is a very common choice for the turbulence-chemistry interaction closure. It has been successfully used in the wide range of applications utilizing MILD conditions; prototype gas turbines employing flameless oxidation [33], pulverized coal combustion in MILD conditions [34, 35, 36], MILD combustion in forward flow furnace of refinery-off gas [37], laboratory scale [38] or semi-industrial flameless furnaces [39] and other kind of MILD combustion devices [40, 41, 42].

However, a commonly reported problem [20, 27, 28, 43, 42, 44, 45] with EDC is that it tends to over-predict the maximum temperature values in the MILD regime. A solution proposed for the problem is to use a strongly modified set of constants for fine structures and residence time. Modification of the EDC model constants was first introduced by Rehm et al. [44], in case of modeling gasification processes. The first modification in MILD regime was proposed by De et al. [27] in the case of Delft Jet-in-Hot-Coflow (DJHC) flame. Later this approach was adopted by other researchers in the case of Adelaide Jet-in-Hot-Coflow (AJHC) [28, 43, 45, 46]. In the work of Graca et al. [42], a numerical simulation of a reversed flow small-scale combustor operating in the MILD regime was performed with modified EDC constants as well. Indeed, simulations with adjusted constants have shown better agreement with the experiment, but questions arise to the generality of this approach. Recently, to overcome that problem, Parente et al. [20] proposed functional expressions for EDC constants dependent on dimensionless flow parameters (Reynolds and Damköhler numbers). They took into account specific features of the MILD combustion mode and applied proposed changes globally and locally. Another recent modification suggested by Aminian et al. [47] was based on a Partially Stirred Reactor (PaSR) to account for finite-rate chemistry in the fine structures. This was related to the local extinction approach previously

studied by Lilleberg et al. [48]. The presence of weak turbulence causes additional difficulties and raises questions on models originally developed for high Reynolds number flows. To account for this problem, De et al. [27] introduced a low Reynolds number limit of validity of EDC, which was later adopted by Shiehnejadhesar et al. [49], who proposed a hybrid EDC/laminar finite rate kinetics model. Recently, Mardani [50] focused on the adjustment of only one of the primary EDC constants from the cascade model [15]. The Jet-in-Hot-Coflow case is closely related to the vitiated coflow or Cabra burner of UC Berkeley. Among the successful RANS simulations of that case is the work of Myhrvold et al. [51] using EDC.

In the present work we analyze and discuss the modifications of EDC constants proposed in recent literature. In spite of a notable number of MILD combustion studies using EDC, and the efforts of modifying it, few or none of those investigators have used EDC in the form originally presented. Rather, a simplification has been used, setting the fraction of reacting fine structures to unity. Therefore, it will be of interest to see the effect of these formulations in MILD combustion. We also study the impact of different formulations of EDC, description of the fine structure reactor and its inflow conditions. The factors that contribute to the increase of the reaction rate in case of low turbulence are identified. Based on the energy cascade model and turbulence closures, we present an alternative approach to avoid the over-estimation problem. Finally, we consider reactivity of the fine structures as the factor that decreases the reaction rates in conditions of non-stoichiometric, incomplete chemical reactions in low-Reynolds-number flows.

The performance of the chosen approaches was assessed on the three flow conditions of DJHC-I flame characterized by a jet Reynolds number of 2500, 4100 and 8800. The calculations have been carried out with the use of open source software OpenFOAM [52] with the EDC model implementation verified and validated previously by Lilleberg et al. [48] and Lysenko et al. [53, 54] in the edcPisoFoam solver. Additionally, we have verified it with the EDC implementation by comparing the results from Ansys Fluent [55] and the edcSimpleSMOKE solver by Cuoci et al. [56]. This analysis provides insight into the use of EDC, which will be useful in the simulations of industrial applications of MILD combustion.

2. Theory and modeling

2.1. Turbulent flow

In order to deal with the problem of turbulent reactive flow, one has to solve the system of closed equations of motion, species transport and energy conservation. In the present work the Navier-Stokes equations are subject to Reynolds decomposition with Favre averaging. The closure for the turbulence fluxes can be obtained by statistical modeling based on turbulence viscosity. The turbulence kinetic energy k and its dissipation rate ϵ are obtained with a two equation k–ϵ turbulence model [57]. The Reynolds stress tensor is calculated according to the Boussinesq hypothesis. The turbulence fluxes of scalars are modeled with the gradient assumption using turbulence Schmidt and Prandtl numbers to estimate respective diffusivities. The key difficulty in mathematical modeling of turbulent combustion is the averaged source term $\bar{R}_k$ in the equation of transport for species mass fraction Y_k, which is treated with a turbulence-chemistry interaction model.

2.2. Eddy Dissipation Concept

The Eddy Dissipation Concept (EDC) of Magnussen represents a turbulent mixing approach of combustion modeling. The idea is that the reactions occur where the reactants are mixed at molecular level and the turbulence energy dissipation takes place; in so called fine structures whose size is of the order of magnitude of the Kolmogorov scales [11, 12, 15]. EDC is based on a cascade model of energy dissipation [15] from larger to smaller scales, so that relations between the scales can be described with a RANS closure, e.g. a k–ϵ model. A control volume is conceptually divided

into fine structures and the surroundings. The role of the cascade model is to represent the information of the fine structures. These are characteristic scales that we cannot calculate, but model with the use of quantities from the mean flow, which are calculated from the turbulence model. It is postulated that the ratio of the mass of regions containing fine structures and the total mass can be expressed as [11, 15]

$$\gamma_\lambda = \left(\frac{3C_{\mathrm{D2}}}{4C_{\mathrm{D1}}^2}\right)^{1/4}\left(\frac{\nu\epsilon}{k^2}\right)^{1/4} = C_\gamma\left(\frac{\nu\epsilon}{k^2}\right)^{1/4} = C_\gamma(Re_\tau)^{-1/4}, \tag{1}$$

where $Re_\tau = k^2/(\nu\epsilon)$ is the turbulence Reynolds number. The constants C_{D1} and C_{D2} occur in the Eddy Dissipation turbulence energy cascade model, which relates the fine structures to the quantities resolved by the turbulence model. Their numerical values were set to $C_{\mathrm{D1}} = 0.135$ and $C_{\mathrm{D2}} = 0.5$ [15]. The mass transfer rate between fine structures and surroundings, divided by the fine-structure mass, is modeled [11, 15] as

$$\dot{m}^* = 2\frac{u^*}{L^*} = \left(\frac{3}{C_{\mathrm{D2}}}\right)^{1/2}\left(\frac{\epsilon}{\nu}\right)^{1/2}. \tag{2}$$

The reciprocal quantity is the mean residence time in fine structures:

$$\tau^* = \frac{1}{\dot{m}^*} = C_\tau\left(\frac{\nu}{\epsilon}\right)^{1/2}. \tag{3}$$

The secondary constants C_γ and C_τ, which are expressed from C_{D1} and C_{D2} as seen in Eqs. (1) and (3), are introduced by some authors for convenience. The standard values lead to $C_\gamma = 2.13$ and $C_\tau = 0.408$.

The relation between the averaged quantities, $\widetilde{\Psi}$, the fine structures quantities, Ψ^*, and the surroundings quantities, Ψ^o, is expressed as a mass-weighted average:

$$\widetilde{\Psi} = \gamma^*\chi\Psi^* + (1-\gamma^*\chi)\Psi^o, \tag{4}$$

where χ is the reacting fraction of the fine structures. According to Magnussen [14], $\gamma^* = \gamma_\lambda^2$ is the mass of fine structures divided by the total mass. In the formulation of Magnussen [12] and Gran and Magnussen [13], γ^* is expressed as γ_λ^3, which resulted from a different interpretation of the shape of turbulence structures. The former corresponds to the Tennekes model [58] of tube-like structures, and the latter to Corrsin's sheet-like structures [15]. Assuming that all the reactions take place only in the fine structures [13], the reaction rate for species k can be calculated from the balance of mass in a homogeneous reactor, which represents the fine structures:

$$R_k^* = \rho^*\dot{m}^*(Y_k^* - Y_k^o). \tag{5}$$

The mean reaction rate is the reacted mass of species k per unit of time per unit volume of the entire fluid in the cell. Including the assumption that only a fraction χ (≤ 1) of the fine structures actually reacts, the mean reaction rate is expressed as

$$\bar{R}_k = \frac{\bar{\rho}\gamma_\lambda^2\dot{m}^*\chi}{1-\gamma^*\chi}({Y_k}^* - \widetilde{Y}_k). \tag{6}$$

For the purpose of further discussions it is convenient to define the EDC factor

$$f_{\mathrm{EDC}} = \frac{\bar{\rho}\gamma_\lambda^2\dot{m}^*\chi}{(1-\gamma^*\chi)}, \tag{7}$$

where the formulation of γ^* differs between [12, 13] and [14] as described above. Introducing the detailed chemical

kinetic approach, the fine structures are treated as a homogeneous reactor, usually isobaric and adiabatic. Then, the mass fractions Y_k^* can be found as a solution of ordinary differential equations describing a perfectly stirred reactor (PSR) or a plug flow reactor (PFR).

In the original EDC formulation, Magnussen [12] and Gran and Magnussen [13] provided functional expressions for χ. They found that for the cases investigated [13], setting $\chi = 1$ gave nearly the same results. Following this, in most instances $\chi = 1$ has been set for simplicity when a detailed chemical mechanism is used. This simplification may not be justified in the non-stoichiometric conditions with low turbulence Reynolds number and incomplete reactions. The reacting fraction of the fine structures, χ, was based on the global one-step irreversible reaction:

$$1 \text{ kg fuel (F)} + \text{r kg oxidant (O)} \rightarrow (1 + \text{r}) \text{ kg product (P)}. \tag{8}$$

The reacting fraction was expressed as $\chi = \chi_1 \cdot \chi_2 \cdot \chi_3$, where

$$\chi_1 = \frac{(\widehat{Y}_{\min} + \widehat{Y}_{\mathrm{P}})^2}{(\widehat{Y}_{\mathrm{F}} + \widehat{Y}_{\mathrm{P}})(\widehat{Y}_{\mathrm{O}} + \widehat{Y}_{\mathrm{P}})} \tag{9}$$

represents the probability of coexistence of the reactants,

$$\chi_2 = \min\Big[\frac{\widehat{Y}_{\mathrm{P}}}{\gamma_\lambda(\widehat{Y}_{\mathrm{P}} + \widehat{Y}_{\min})}, 1\Big] \tag{10}$$

expresses the degree of heating, and

$$\chi_3 = \min\Big[\frac{\gamma_\lambda(\widehat{Y}_{\mathrm{P}} + \widehat{Y}_{\min})}{\widehat{Y}_{\min}}, 1\Big] \tag{11}$$

is limiting the reaction due to lack of reactants. The quantities $\widehat{Y}_{\mathrm{F}}$, $\widehat{Y}_{\mathrm{O}}$, $\widehat{Y}_{\mathrm{P}}$ and $\widehat{Y}_{\min}$ are scaled mass fraction according to the stoichiometry of the reaction in Eq. (8):

$$\widehat{Y}_{\mathrm{F}} = \frac{\widetilde{Y}_{\mathrm{F}}}{1}, \quad \widehat{Y}_{\mathrm{O}} = \frac{\widetilde{Y}_{\mathrm{O}}}{\mathrm{r}}, \quad \widehat{Y}_{P} = \frac{\widetilde{Y}_{\mathrm{P}}}{1 + \mathrm{r}} \quad \text{and} \quad \widehat{Y}_{\min} = \min\{\widetilde{Y}_{\mathrm{F}}, \widetilde{Y}_{\mathrm{O}}\}. \tag{12}$$

The DJHC burner was fuelled with Dutch natural gas. The main component was methane, which played the main role in the global stoichiometry. Therefore, in this work $\widetilde{Y}_{\mathrm{F}}$ and $\widetilde{Y}_{\mathrm{O}}$ are the mass fractions of methane and oxygen, respectively; accordingly, $\mathrm{r} = 4.0$. $\widetilde{Y}_{\mathrm{P}}$ is the sum of the mass fractions of water vapor and carbon dioxide, here including diluents from the coflow.

2.3. Fine structure reactor

2.3.1. Perfectly stirred reactor

Gran and Magnussen [13] took into account the effects of finite-rate chemistry by describing the fine structures as transient perfectly stirred reactors. The set of ordinary differential equations are in the following form [13]:

$$\frac{dY_k^*}{dt} = \frac{R_k^*}{\rho^*} + \frac{1}{\tau^*}(Y_k^o - Y_k^*). \tag{13}$$

Fluid entering the reactor has the properties of the surroundings, whereas the outflow has the fine-structures properties, and the mixing rate is equal to $1/\tau^*$. Equation (13) is integrated in time to achieve a steady state solution [13, 53]. This kind of stiff, highly non-linear set of Ordinary Differential Equations (ODE) needs to be solved with a robust algorithm. However, as reported by Shiehnejadhesar et al. [49], the PSR approach may lead to convergence problem

during the iterative solution. Therefore, in order to simplify the numerical solution process, the PFR is often used instead of PSR.

2.3.2. Plug flow reactor

The plug flow reactor is a one-dimensional, steady state reactor with inflow and outflow, and a field of properties along the flow direction. In this approach reactions proceed over the time scale τ^*, governed by Arrhenius reaction rates [27, 49, 55]. With constant flow velocity, area and pressure, the governing balances can be transformed into transient equations, for instance the species mass balance:

$$\frac{dY_k}{dt} = \frac{R_k^*}{\rho^*} \tag{14}$$

In the case of the Ansys Fluent implementation of EDC, initial conditions are taken as the current mean values of species mass fractions and temperature in the cell [55], which means that Eq. (14) is integrated from $Y_k(t=0) = \widetilde{Y}_k$ to $Y_k(t=\tau^*) = Y_k^*$.

2.4. Discussion of the fine structure reactor

Although the two approaches are quite similar, the use of mean values instead of surroundings as the initial (inflow) conditions has considerable implications for the low turbulence flows. When the PSR is assumed to approach steady state, the balance Eq. (13) can be written as:

$$(Y_k^* - Y_k^o) = \frac{R_k^*}{\rho^*}\tau^*. \tag{15}$$

Similarly, from the PFR, Eq. (14), we can obtain

$$(Y_k^* - \widetilde{Y}_k) = \int_0^{\tau^*} \frac{R_k^*}{\rho^*} dt \approx \frac{R_k^*}{\rho^*}\tau^*. \tag{16}$$

It can be shown that if the inflow/initial conditions are the same, then the solution of the PSR and PFR gives comparable results. This has also been reported by other researchers [49, 59] and was confirmed with the simulations in Ansys Fluent and edcSimpleSMOKE. However, conditions are different in this case. When the mean value is used, the fine structure mass fraction is simply $Y_k^* = R_k^*\tau^*/\rho^* + \widetilde{Y}_k$, and when the surroundings value is used, taking into account Eq. (4), it becomes $Y_k^* = (1-\gamma^*\chi)R_k^*\tau^*/\rho^* + \widetilde{Y}_k$. This means that in the former case, the mass fraction Y_k^* of the species k produced in the fine structures is always smaller than if the surroundings value is used. Therefore, the ratio of the two mean reaction rates obtained with the two approaches can be expressed as:

$$\frac{\bar{R}_{k,mean}}{\bar{R}_{k,surr}} = \frac{R_k^*\tau^*/\rho^*}{(1-\gamma^*\chi)R_k^*\tau^*/\rho^*} = \frac{1}{1-\gamma^*\chi}. \tag{17}$$

For high Reynolds numbers, the ratio is close to unity. However, at low Reynolds number, γ^* can have notable values resulting in the ratio higher than unity. That means over-predicted values of reaction rate in PFR/PSR approach with the mean value used as initial/inflow condition. It can be also shown that the difference between the formulation of Magnussen [14] and Gran and Magnussen [13] exist only in the case when the mean value is used as the PFR inlet. It results from the uncompensated ratio of the EDC factors of the two versions, which can be written as

$$R_{edc} = \frac{1-\gamma_\lambda^3\chi}{1-\gamma_\lambda^2\chi}. \tag{18}$$

It takes values between 1 and 1.5 in the range of $\gamma_\lambda \in (0,1)$, which means that the EDC factor, Eq. (7) in the formulation of Magnussen [14] is always slightly higher.

At this point it should also be noted that the EDC validity limit of turbulence Reynolds number of 64 presented by De et al. [27], and later considered by Shiehnejadhesar et al. [49] and mentioned by Mardani [50], is restricted to the special implementation of EDC adopted in Ansys Fluent. It is not a limit of validity for EDC in general. Very recently, this issue was also partially raised by Li et al. [60]. The limit was introduced [27] by the comparison of two time scales: τ^* and the characteristic time scale of the linear relaxation process of the order of the time scale of the energy containing scales of turbulence, τ_{mix},

$$\frac{1}{\tau_{mix}} = \frac{1}{\tau^*}\frac{\gamma_\lambda^2\chi}{(1-\gamma_\lambda^3\chi)}. \tag{19}$$

This expression is the EDC factor f_{EDC}, Eq. (7), divided by $\bar{\rho}$. Therefore, the mean and the fine structure reaction rate, Eqs. (6) and (14), could be written as

$$\bar{R}_k = \frac{\bar{\rho}}{\tau_{mix}}(Y_k^* - \widetilde{Y}_k) \quad \text{and} \quad R_k^* = \frac{\rho^*}{\tau^*}(Y_k^* - \widetilde{Y}_k). \tag{20}$$

De et al. [27] inferred that the mixing time scale τ_{mix} should be greater than the fine-structure time scale τ^*. Hence, a ratio of the two scales needed to be less than unity,

$$R = \frac{\tau^*}{\tau_{mix}} = \frac{\gamma_\lambda^2\chi}{(1-\gamma_\lambda^3\chi)} < 1. \tag{21}$$

From this relation it followed that $\gamma_\lambda < 0.75$ and, therefore, $Re_\tau > 64$ (accordingly $\gamma_\lambda < 0.707$, $Re_\tau > 84$ in formulation of Magnussen [14]) for the cases when $\chi = 1$. However, in the original formulation of the EDC, a PSR approach was used with the surroundings value of the mass fraction as the inflow condition described in Eqs. (5) or (15). In such a case, with the use of the relation of Eq. (4), the two reaction rates can be expressed as

$$\bar{R}_k = \frac{\bar{\rho}\gamma_\lambda^2\chi}{\tau^*}(Y_k^* - Y_k^o) \quad \text{and} \quad R_k^* = \frac{\rho^*}{\tau^*}(Y_k^* - Y_k^o), \tag{22}$$

where $\tau_{mix} = \tau^*/\gamma_\lambda^2\chi$, thus equivalent time scale ratio leads to the trivial requirement:

$$R = \frac{\tau^*}{\tau_{mix}} = \gamma_\lambda^2\chi < 1. \tag{23}$$

If $\chi = 1$, $\gamma_\lambda < 1$, which corresponds to the turbulence Reynolds number higher than 21. At lower values of Re_τ, γ_λ will need a modification, as attempted and investigated by Myhrvold [61] for the case of a near-wall layer. However, approaching the limit of low Reynolds number, it should be noted that the cascade model of EDC was developed under the assumption of a "high" Reynolds number. At very low Reynolds numbers, the cascade will be reduced, what might lead to different secondary constants values C_γ and C_τ. However, both constants will slightly increase, which is in conflict with a suggestion of decrease in C_γ value for MILD regime [27, 28, 43].

2.5. Modified model constants from the literature

In the first modification of the EDC constants in gasification modeling, Rehm et al. [44] tried larger values of both C_γ and C_τ (trials up to 13.0 and 8.0, respectively). In the case of DJHC flame, De et al. [27] suggested to increase C_τ to 3.0 or decrease C_γ to 1.0. Later, different combinations of the modified constants were also tested on the AJHC flame [28, 43, 45, 46]. As a theoretical reason to support the changes of the constants, it was argued that in the

MILD regime, reaction rates are slower, thus increase in C_τ, and it is characterized by relatively broad reaction zones, thus changes in C_γ. Graca et al. [42], based on their experience on a reversed flow small-scale combustor operating in MILD regime, claimed a minor influence of change in the C_τ value. Unlike the previous works, they increased C_γ to the value of 5.0. Nevertheless, the change in the two parameters, which are interpreted as a time scale and fine structure constants due to the specific features of MILD combustion, seems reasonable. However, the survey of proposed new modified values reflects some disagreement and the uncertainty of the exact choice, which causes lack of generality of such approaches. To overcome that problem, Parente et al. [20] recently proposed a more sophisticated procedure for the estimation of the EDC constants where they depend on two dimensionless parameters: turbulence Reynolds number and Damköhler number. Their main assumption was to interpret u^* as the characteristic speed of the turbulent reacting fine structures and to approximate it by the turbulent flame speed S_L. In this extension the quantities C_γ and C_τ were not constants anymore but functional expressions providing values in a certain range. However, these considerations concerned only its impact on the reaction rate itself, whereas modified constants have implications in the experiments they were originally derived from. Therefore, constants modifications should be also discussed in the relation with the dissipation model and turbulence in the equilibrium zone of a boundary layer. As presented in Eqs. (1) and (3), the single-symbol constants C_γ and C_τ were introduced for convenience. The primary constants C_{D1} and C_{D2} may be retrieved as

$$C_{D1} = \frac{3}{2}\frac{C_\tau}{C_\gamma^2} \quad \text{and} \quad C_{D2} = 3C_\tau^2. \tag{24}$$

It should be noted that C_γ affects only C_{D1}, whereas a change in C_τ has an effect on both C_{D1} and C_{D2}. Recently, Mardani [50] focused on the modification of only C_{D2} constant in order to adjust the model to MILD conditions.

The constants C_{D1} and C_{D2} of the cascade model were adapted to experimental data of turbulent flows [15, 62]. The C_{D1} was calibrated on the same equilibrium boundary layer data that were used to settle the values of C_μ in the k–ϵ model [57] and β^* in the k–ω model [63, 64]. The value of C_{D1} corresponds to three-half of C_μ or β^*, which both were set to the square root of a value 0.3 for the ratio of turbulence shear stress to turbulence energy. The value 0.3 can be discussed, however, said models have had an undeniable success. Minor departures from these data, such as a slightly lower C_μ used in the RNG k–ϵ model [65] is not likely to cause significant problems. However, large modifications to C_{D1} will introduce an inconsistency between cascade model and turbulence model. Suggestions in literature include values like $C_{\mathrm{D1}} \approx 0.6$ (resulting from $C_\gamma = 1.0$ [27, 28, 43]), $C_{\mathrm{D1}} \approx 1$ (from $C_\tau = 3.0$ [27, 28]), $C_{\mathrm{D1}} \approx 2.4$ ($C_\gamma = 0.5$ [28]), and $C_{\mathrm{D1}} \approx 0.06 - 0.004$ ($C_\gamma = 3.2 - 13$ [44]). The second constant, C_{D2}, was related to decaying turbulence and the ratio of kinetic energy transfer to smaller scales to the viscous dissipation [15, 66]. Mardani [50] pointed out that C_{D1} should not be changed to preserve consistency with a turbulence model. Taking above discussion into account this suggestion can be extended to C_{D2} so that both values should be kept constant. The proposed [50] value of $C_{\mathrm{D2}} = 0.0239$ led to a simultaneous decrease of C_τ and C_γ, that contradicted to the previous studies [27, 28]. A change in C_τ to the value of an order of magnitude lower than the standard value will increase the reaction rate in case of DJHC flame.

3. The test case and boundary conditions

In the present study the test case that emulates MILD regime was the Delft Jet-in-Hot-Coflow (DJHC) burner [7] for which, in contrast to the Adelaide Jet-in-Hot-Coflow (AJHC) [8], are available velocity measurements but not species mass fraction data. The configuration of the DJHC burner is presented in Fig. 1 and consisted of a central primary fuel jet with 4.5 mm inner diameter, surrounded by an annular coflow of diameter 82.8 mm. The coflow stream was generated by a partially premixed combustion of the same fuel. A series of experiments with several fuel

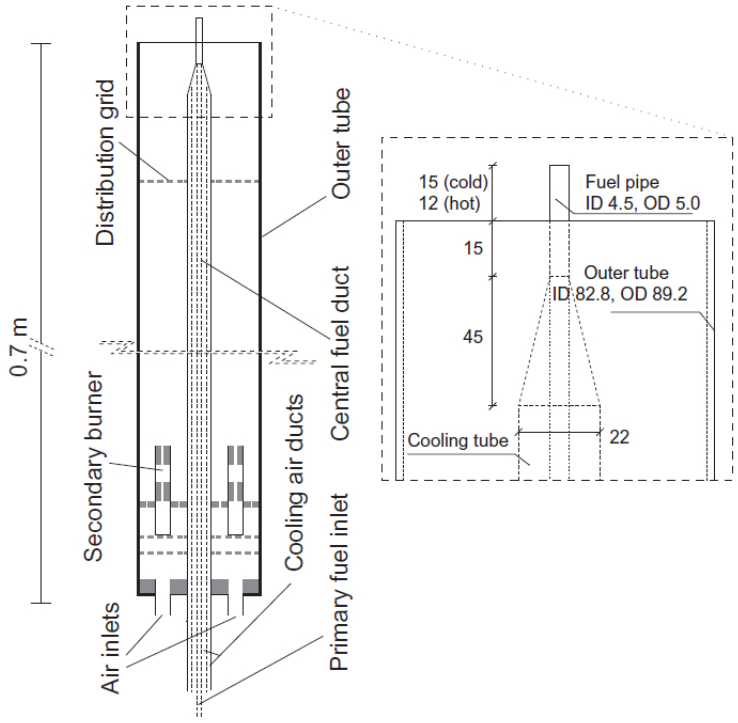

Figure 1: Schematic design of the Delft Jet-in-Hot-Coflow burner [7].

mass flow rates, and different types of coflow varied by oxygen content, temperature and mass flow rate, were carried out by Oldenhof et al. [7]. In the present modeling study, the flame denoted as DJHC-I-S [7, 27] was considered with three different fuel mass flow rates resulting in jet Reynolds numbers of 2500, 4100 and 8800 (see Table 1). The composition of the Dutch natural gas was specified as 15 % N_2, 81 % CH_4, 4 % C_2H_6 (by volume), with coflow flue gases considered as products of its combustion with oxygen content of 7 % and the remaining species calculated with an equilibrium assumption as suggested by De et al. [27] (6 % CO_2, 12 % H_2O, 74.5 % N_2 by volume and other minor species, including OH).

In the simulations of AJHC burner, Christo and Dally [18] and Frassoldati et al. [67] pointed out that the numerical solution was sensitive to the turbulence level at the inlets. However, they did not have access to the experimental inlet data and had to perform cold flow simulations inside the burner [18] or use pre-inlet pipe [67] and make some adjustments of the turbulence quantities to obtain correct jet spreading rate. Thus variations of k of two orders of magnitude had significant meaning.

The inlet boundary conditions for temperature and velocity profiles were taken from experimental data measured at locations 3 mm above the jet exit. The turbulence kinetic energy profile was calculated from the measured axial and

Table 1: Characteristics of the DJHC-I flames with different Reynolds numbers for the fuel jet and coflow streams.

	Fuel jet			Coflow		
Jet Reynolds number	T_{min} [K]	U_{max} [m/s]	$\dot{V}$ [normal l/min]	T_{max} [K]	U_{max} [m/s]	$\dot{V}$ [normal l/min]
2500	460	25.5	10.7	1536	4.9	240.1
4100	448	33.9	16.1	1540	4.6	240.1
8800	462	56.8	30.0	1538	4.9	240.1

radial normal components of the Reynolds stresses, while assuming that the azimuthal component $\widetilde{w'w'}$ was equal to the radial $\widetilde{v'v'}$, as proposed by De et al. [27]. The inlet mean turbulence energy dissipation rate profile was estimated by assuming that it was equal to the turbulence energy production. Alternatively, this method can be extended even if the Reynolds stresses are unknown, using expressions for k and ϵ derived by Lewandowski et al. [68]. For the tunnel air no detailed measurements were available, thus the uniform values of temperature and velocity equal to 293 K and 0.5 m/s were taken, respectively.

It is worth mentioning that a recently presented new MILD combustion definition, based on an equivalent activation energy [69] and further observations [70], suggested that DJHC flames do not fully meet criteria for MILD combustion. However, the classical definition [4] is fully satisfied, as the inlet temperature of the reactant mixture is higher than mixture self-ignition temperature and the increase in the temperature during the combustion is low. An oxygen content in the coflow stream below 8 % also places said flames in the MILD combustion regime, as suggested e.g. by Sidey and Mastorakos [71].

4. Numerical simulation

The most popular numerical code with implementation of EDC seems to be Ansys Fluent [55], which has a huge advantage of use of the ISAT algorithm [72] to accelerate the calculations. However, the graphical user interface allows to configure the model only through the C_γ and C_τ constants. On the other hand, the open source computational code OpenFOAM, which became a favorable choice in the academic community, has a huge potential in the industrial applications as well. We have used two OpenFOAM solvers edcPisoFoam and edcSimpleSMOKE. We have assessed and verified them with Ansys Fluent and obtained a relatively good agreement in the resuls between all the codes. Some discrepancies in the velocity distributions due to the turbulence modeling were observed. This was evidenced by a different jet spreading rate in the results from Ansys Fluent and OpenFOAM. Also the turbulence Reynolds number in case of Ansys Fluent was higher than in OpenFOAM. It was observed that the character of f_{EDC} distribution in the two codes was very similar but the values were always slightly higher in case of Ansys Fluent. This resulted in somewhat higher temperature values when the latter code was used. Nevertheless, most of the further investigations have been carried out with the modified edcPisoFoam solver. In order to obtain a proper flow field, we have first focused on accurate turbulence closure approaches and have assessed six versions of the k–ϵ model run in the case of DJHC at $Re = 4100$. Several variants of the model were tested: standard [57], modified $C_{\epsilon 1}$ [73], realizable [74], Renormalization Group (RNG) [65], Launder and Sharma [75] and Pope [76]. It is a widely used practice to modify value of $C_{\epsilon 1}$ to 1.6 for a round jet. The reason behind this is over-predicting the decay rate and the spreading rate of a round jet flow [77] in the standard formulation. The version of Launder and Sharma and that with modified $C_{\epsilon 1}$ highly over-predicted the velocities in the central positions of the jet, while suddenly under-predicting it in the outer part of the jet and giving a good agreements with the experiment in the outer coflow region. The former is a low Reynolds number model, however, developed for the purposes of the near wall region modeling. It seemed not to work well in cases of jet flames with a low turbulence Reynolds number. It should be noted that round jets accompanied by a strong coflow are likely to have a longer potential core [78]. In case of DJHC flames this fact was pointed out in [68]. Nathan et al. [79] reported that besides the known effect of the jet entrainment decrease due to combustion, the presence of the coflow additionally enhances this reduction. Moreover, the coflow also reduces the mean spreading rate and the decay of jet centerline velocity. This effect, together with the reported observation that the decay rate reduces with the decreased jet Reynolds number, could be responsible for the fact that the $C_{\epsilon 1}$ correction seems not to be applicable to (at least), the two DJHC flames with lower Reynolds number. For the case of $Re = 4100$ there were only small differences between the distributions obtained with the standard, realizable and RNG k–ϵ model, from

which, however, the standard version of the model appeared to give the most satisfactory results. This observation was consistent with Labahn et al. [31], who also used OpenFOAM. Therefore, for further investigations of flames with the jet Reynolds number 2500 and 4100 the standard formulation of k–ϵ was used (see Fig. 2). However, for the case with the higher Reynolds number of 8800, some turbulence model adjustment was needed. For that purpose we found the Pope correction [76] to be the most appropriate. Thus, for the simulations of the higher Reynolds number case we modified the ϵ equation by adding the term as proposed in [76]. For the clarity Fig. 2 shows only the results obtained with the standard k–ϵ, modifed $C_{\epsilon 1}$ and the Pope correction.

In MILD combustion, due to the diluted conditions, radiative fluxes can be significantly different from conventional combustion processes. Therefore, proper radiation modeling would be desired. However, Christo and Dally [18] presented that there was no noticeable effect on the solution of AJHC flame with the use of discrete ordinate (DO) radiation model [80] in conjunction with WSGGM. De et al. [27] also checked the DO method as well as the P1 radiation model in the case of DJHC and reported that the maximum temperature difference between the calculations with and without radiation effects was about 50 K. This observation was also confirmed in our calculations with Ansys Fluent. In the current study we wanted to focus on the impact of the EDC model parameters. Therefore the effect of radiation was of secondary importance, and the further simulations were performed without taking it into account.

Christo and Dally [18] reported that differential diffusion effects played an important role in MILD combustion regime. They were, however, considering AJHC burner, which was fueled with a mixture containing a considerable amount of hydrogen. In case of the present study, the DJHC burner was fueled with the Dutch natural gas with no hydrogen. De et al. [27] reported negligible effects of differential diffusion. Therefore, in our simulations the diffusion coefficient was set equal for all species, $D_i = 2.88 \cdot 10^{-5} \mathrm{m}^2/\mathrm{s}$. The molecular viscosity was calculated according to the Sutherland law. Turbulence Prandtl and Schmidt numbers were set to 0.85 and 0.72, respectively. The gravitational acceleration was taken into account for the vertical momentum equations in all the simulations, as it was especially important in the coflow region.

In all the simulations, the DRM19 chemical mechanism [81] was used. This is a reduced reaction set based on GRI-Mech 1.2, comprising 19 species and 84 reactions. It is noted that there is some discussion on whether standard chemical mechanisms can be used for MILD combustion, as they are required to work outside the conditions for their optimization [82, 83]. Ongoing research aims at reliable models for MILD combustion chemistry. Alternatively, existing models might be improved, cf. Tu et al. [84]. However, the DRM19 mechanism appeared to perform sufficiently well in previous studies of the DJHC flame [27, 85].

A computational domain was set up similar to the one in the study of De et al. [27]. An axisymmetric two-dimensional configuration was used. Inlet conditions as described in Section 3 were derived from experimental data measured 3 mm above the jet exit. Therefore, the grid began at this location and extended 225 mm in axial and 80 mm in radial direction. A grid independence study of five different mesh sizes (9000, 10800, 16200, 22500 and 45000 cells) allowed us to use the grid that consisted of 180 cells in axial direction and 60 cells in radial directions (10 for the fuel inlet, 35 for the coflow and 15 for the ambient air). OpenFOAM used a collocated grid arrangement with the Rhie-Chow interpolation [86]. The PISO algorithm for the pressure-velocity coupling and second-order accuracy schemes were used for spatial discretization. The edcPisoFoam solver was designed for transient problems but, since we were aiming at a steady-state solution, we used a first-order implicit Euler method for the time derivative. Integration of the stiff ordinary differential equations of the perfectly stirred reactor was performed with the RADAUA5 algorithm [87]. Results are plotted against experimental data [7] with RMS values as the “error bars” for the temperature distributions.

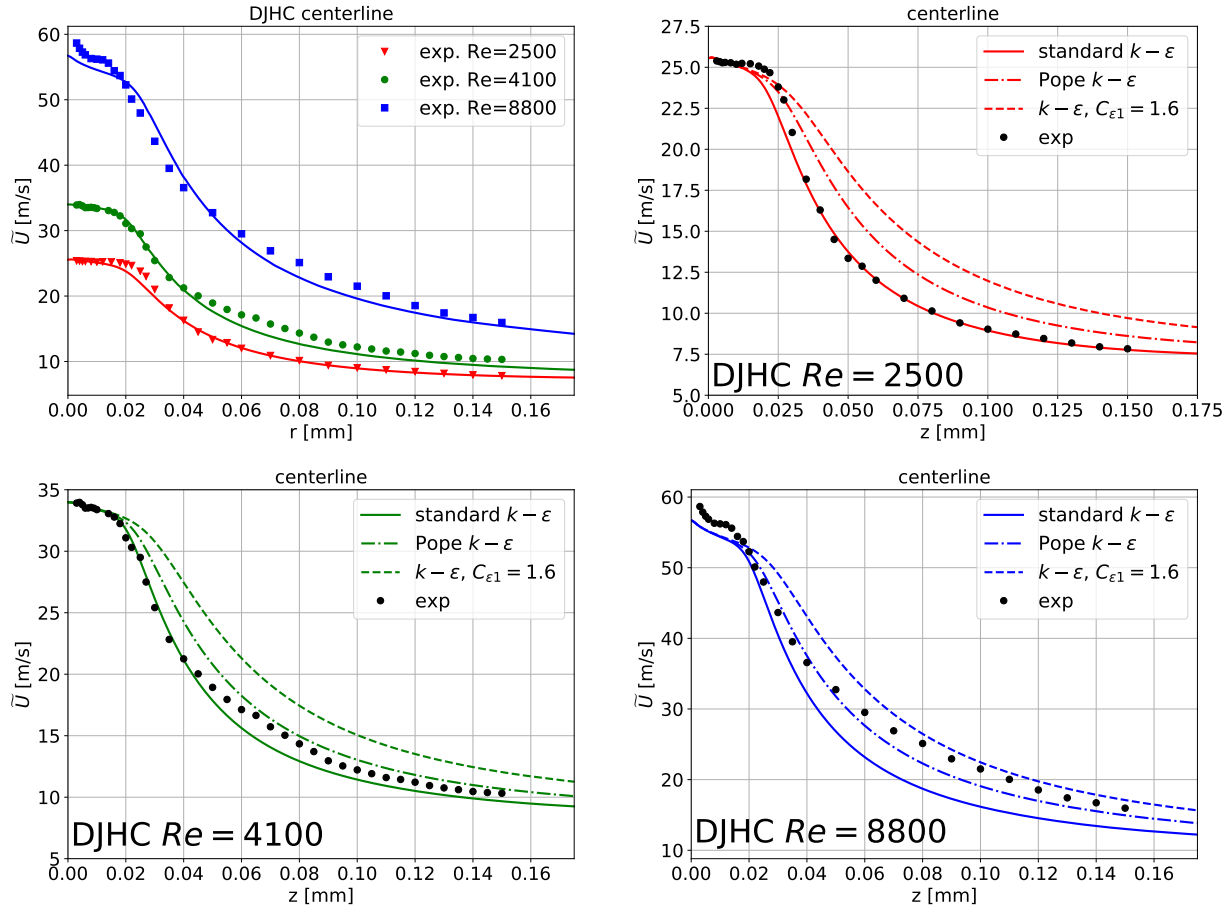

Figure 2: The axial profiles of the mean streamwise velocity for the flame DJHC-I at $Re = 2500$ (red), $Re = 4100$ (green) and $Re = 8800$ (blue). Symbols represent the experimental data and lines represent simulations obtained with the three variants of the k–ϵ model. In the first plot, results of $Re = 2500$ and $Re = 4100$ were obtained with the standard k–ϵ model, whereas for the case $Re = 8800$ Pope correction was applied.

5. Results and discussion

5.1. Impact of the EDC formulation

As discussed in Section 2.4, several ways of formulating EDC exist in the literature, among which some are not fully consistent with the theory. In Table 2 nine different formulations are reported according to the EDC factor f_{EDC} (Eq. (7)), PSR inlet value and the limit of γ_λ. The numbers 1 and 2 in the case identifiers denote formulation of EDC according to Magnussen [14] and Gran and Magnussen [13], respectively. Cases with a character A concern situations when the surroundings values of species mass fractions were used as the inlet values to the PSR and γ_λ needed to fulfill a trivial requirement $\gamma_\lambda < 1$ which was discussed in Section 2.4. In the Cases B, the mean values of species mass fractions were used as the PSR inlet, and γ_λ was clipped for values higher than 0.7 and 0.75 (for Cases 1 and 2, respectively), according to Eqs. (23) and (21) (with $\chi = 1$). Cases D and E are other combinations, namely; mean values were used as the PSR inlet, and no γ_λ clipping was applied for Cases D. For Cases E, surroundings values were used as the PSR inlet, and clipping of γ_λ was applied. Case C was formulated so that the mean reaction rate was derived again taking into account the use of the mean value as the inflow to the steady PSR, so that the denominator $(1 - \gamma^*\chi)$ was not present in the EDC factor f_{EDC}. The other cases applied Eq. (7).

In Fig. 3 Cases A1, A2, B1 and B2 are compared to show the impact on temperature due to the differences in

reaction rates obtained with the formulation of Magnussen [14] and Gran and Magnussen [13] as discussed in Section 2.4 and expressed in Eq. (18). As predicted there were no differences between Cases A1 and A2, yet there were discrepancies between Cases D1 and D2 showing that the formulation of Magnussen [14] slightly over-predicted the reaction rate only in the case when the mean value was used as the inflow condition. Interesting is the fact that Case C gave better results than the previous cases.

Case B2 represents the implementation used in Ansys Fluent with the formulation of Gran and Magnussen [13], the mean value as the PFR initial condition and clipping $\gamma_\lambda < 0.75$. As presented in Section 2.4, and reported by Shiehnejadhesar et al. [49], solution of ODE in the form of PSR and PFR returns comparable results, so this difference can be treated as negligible. However, the impact of mean value initial/inflow condition and clipping should be taken into account. To distinguish the two effects, the additional Cases D (inflow) and E (clipping) were performed. Temperature results from Cases A2, B2, D2 and E2 (with formulation of Gran and Magnussen [13]) are summarized in Fig. 4. If we compare now temperatures in Case A2 and D2, we can see that not only the temperature is higher in case D2 but observed is also a large decrease in a lift-off height as evidenced by a temperature peak in tha radial distribution at position $z = 15$ mm. That confirms a higher reaction rate if the mean value is used and presents its separated impact on the results. Comparison of Cases A2 and E2 provided information on the impact of clipping γ_λ, which significantly reduced the maximum temperature. Therefore, we can expect that the two combined effects may give something in between. This was confirmed by the results of Case B2. Yet it can be observed that the effect of clipping was much stronger than the effect of inflow condition.

5.2. Reacting fraction χ

In this section the influence of the reacting fraction χ is discussed, cf. Eqs. (4) and (6). The unity value of χ was shown [13] to give approximately the same results as with the use of functional expressions in the case of a bluff-body stabilized diffusion flame. This practice is simpler to implement, and setting $\chi = 1$ has been widely adopted for use of EDC with detailed chemistry. Gran and Magnussen [13] presented that the fraction of fine structures where reactions occur is a product of the probability of coexistence of the reactants. In cases of a non-stoichiometric local mixture and of incompleted reactions, the value of χ will be less than unity. It also includes some effects of Re_τ.

Moreover, Evans et al. [70] recently presented effects of oxidant stream composition on non-premixed laminar flames with heated and diluted coflows to provide insight into the chemical structure of flames in MILD conditions. They concluded that the intensity of MILD reaction zones was strongly dependent on the coflow composition. It concerned especially concentrations of CO_2 and equilibrium OH, which influenced different chemical pathways. The effect of reduced reactivity due to increased concentration of CO_2 in the AJHC flames emulating MILD conditions was also

Table 2: Different formulations of the EDC reaction rate; 1 denotes formulation of Magnussen [14], 2 denotes formulation of Gran and Magnussen [13] and Case C corresponds to EDC factor equal to $f_{\mathrm{EDC}} = \bar{\rho}\gamma_\lambda^2\dot{m}^*$. Calculations were performed with edcPisoFoam solver.

case	f_{EDC}	PSR inlet value	$\gamma_\lambda <$
A1	$\gamma^* = \gamma_\lambda^2$	surroundings, Y_k^o	1
A2	$\gamma^* = \gamma_\lambda^3$	surroundings, Y_k^o	1
B1	$\gamma^* = \gamma_\lambda^2$	mean, $\widetilde{Y}_k$	0.7
B2	$\gamma^* = \gamma_\lambda^3$	mean, $\widetilde{Y}_k$	0.75
C	$f_{\mathrm{EDC}} = \bar{\rho}\gamma_\lambda^2\dot{m}^*$	mean, $\widetilde{Y}_k$	1
D1	$\gamma^* = \gamma_\lambda^2$	mean, $\widetilde{Y}_k$	1
D2	$\gamma^* = \gamma_\lambda^3$	mean, $\widetilde{Y}_k$	1
E1	$\gamma^* = \gamma_\lambda^2$	surroundings, Y_k^o	0.7
E2	$\gamma^* = \gamma_\lambda^3$	surroundings, Y_k^o	0.75

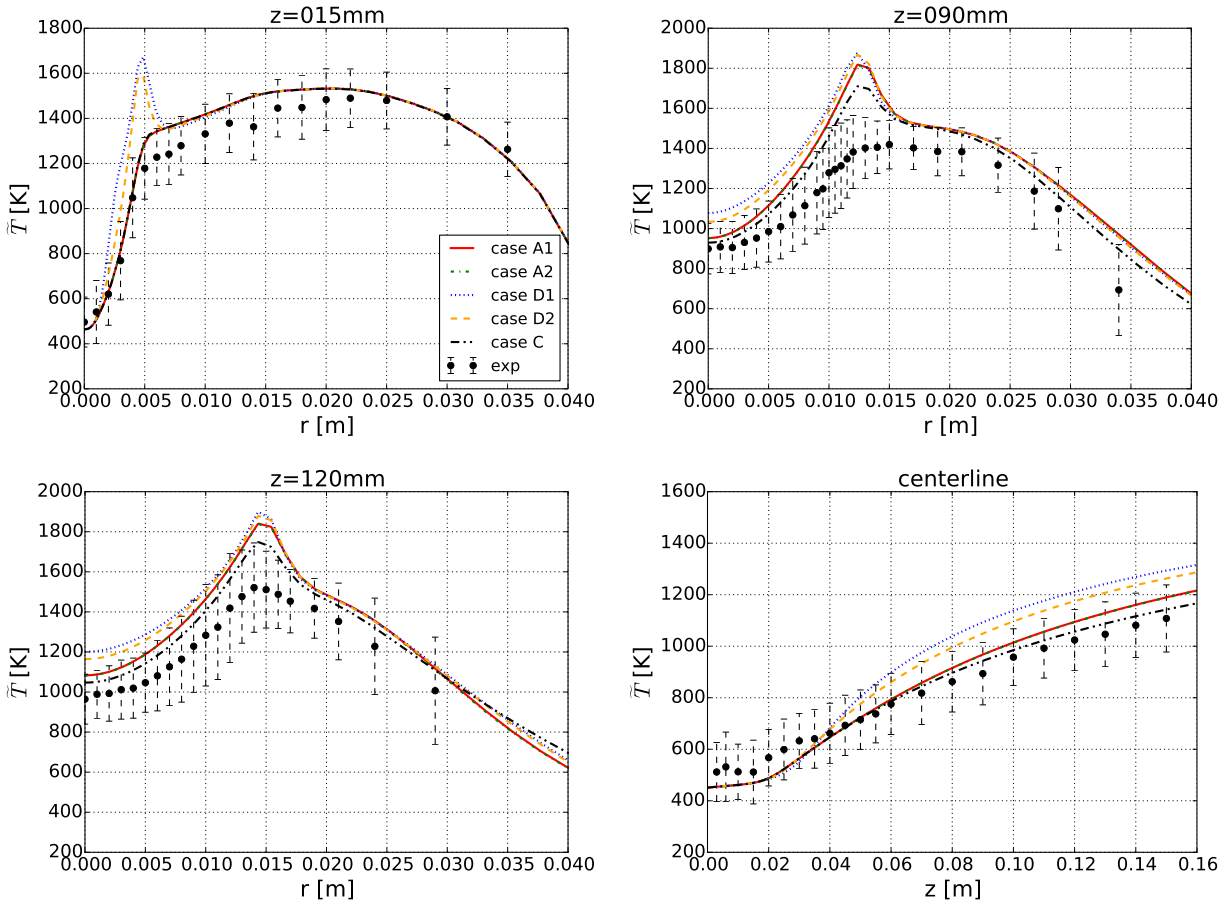

Figure 3: The temperature distribution for the flame DJHC-I-S $Re = 4100$ for the centerline and the radial positions; 15 mm, 90 mm and 120 mm downstream of the nozzle. Comparison of simulations performed in the formulation of Magnussen [14] with Gran and Magnussen [13] in two cases: when mean or surrounding value is used as the inflow condition to the PSR. The fifth simulation represents the case when the mean value is used but the factor $(1-\gamma_\lambda)^{-1}$ is not introduced.

reported earlier by Tu et al. [46], who used EDC with modified constants. In this case, the observed effect was also caused mainly by the chemistry, with some minor influence of physical properties of carbon dioxide.

It is useful to analyze the impact of χ as it reduces the overall reaction rates by decreasing the reaction rates in the fine structures. Figure 5 shows results obtained with selected constant values of χ varying from 1.0 to 0.5. It is clearly seen that with the decreased value of χ, the temperatures were reduced as well. It is worth noticing that every value of χ lower than unity contributes to vanishing the temperature peak in the radial distribution at location 30 mm and, accordingly, every value lower than 0.9 at the location 60 mm. In this case, values of $\chi \leq 0.5$ led to extinction of the flame. Apparently, the unity value of χ was not appropriate for this case. The task remains to figure out whether the formulation of [12, 14] or [13] will be sufficient or if, for instance, including a relation to the Damköhler number (cf. Parente et al. [20]) will improve the model.

It should be noted, that the expressions of χ in Eqs. (9)-(11) are functions of γ_λ. Thus, the clipping of γ_λ mentioned above will have an impact on χ. Without clipping, the lift-off height increased substantially. The radial profile of temperature was lowered significantly in the upstream part of the jet, but less in the downstream part ($z > 120$ mm). The approach of a variable χ calculated without limit on γ_λ (Eqs. (9)-(11)), although clipping γ_λ to 0.7 when used in the EDC factor (Eq. 7), was found to be the most appropriate. Radial distributions of the factors of χ at the location $z = 90$ mm are presented in Fig. 6(left). First, it is clearly seen that the value of χ_3 was constant and equal to one

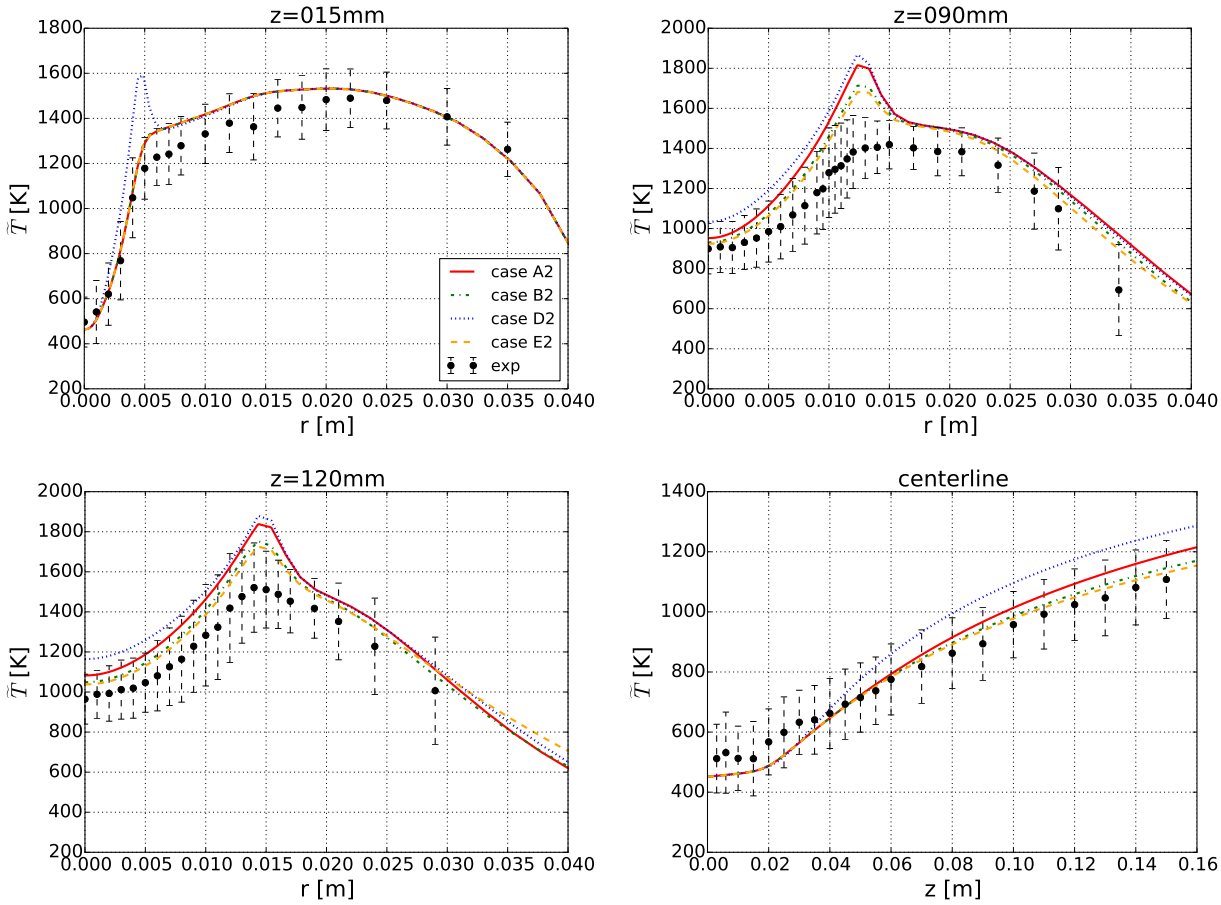

Figure 4: The temperature distribution for the flame DJHC-I-S $Re = 4100$ for the centerline and the radial positions; 15 mm, 90 mm and 120 mm downstream of the nozzle. Comparison of simulations performed in the formulation of Gran and Magnussen [13] in four cases: when mean or surrounding value is used as the inflow condition to the PSR, with and without clipping of γ_λ value.

across the flame. This is reasonable from Eq. (11), as for high values of γ_λ, $\widehat{Y}_{\min}$ rarely is higher than $\widehat{Y}_{\rm P}$. The factor χ_2 can have a value lower than unity when γ_λ is above 0.5, while $\widehat{Y}_{\rm P}$ is less than $\widehat{Y}_{\min}$ by a factor of $\gamma_\lambda/(1-\gamma_\lambda)$. The behavior of χ_1 is different as it achieves unity value only at the location of stoichiometry, $\widehat{Y}_{\min} = \widehat{Y}_{\rm F} = \widehat{Y}_{\rm O}$, and everywhere else it is lower than that. It formed a sharp peak value as seen in Fig. 6 (left).

The grid independence study (Section 4) was performed with the simulation where $\chi = 1$. However, for a variable χ a finer mesh may be needed. Accordingly, simulations with variable χ were repeated on the 45000 cell grid (denoted as M2). Additionally, values of χ_1 were forced to unity when $|\widehat{Y}_{\rm F} - \widehat{Y}_{\rm O}| < 0.01$, in order to ensure a proper peak. Using variable χ effectively decreased the temperature for the cases considered, although for the flame at Re=8800, the improvement was less significant. Results of the simulations with the formulation of Magnussen [14] with $\chi = 1$, and of simulations with variable χ are presented in Fig. 6 (right) for the radial position z=90 mm. The results obtained with variable χ are presented together with other approaches in Fig. 7 and discussed in the next section.

5.3. Comparison of selected approaches on the two flow conditions

Finally, we compared the proposed and discussed approaches on the basis of the three jet Reynolds numbers 2500, 4100 and 8800. We compared simulations with few different settings. The reference simulation, denoted as BFM2005, applied the formulation as in Case A1, i.e. that of Magnussen [14] with the use of surroundings value as inlet to PSR,

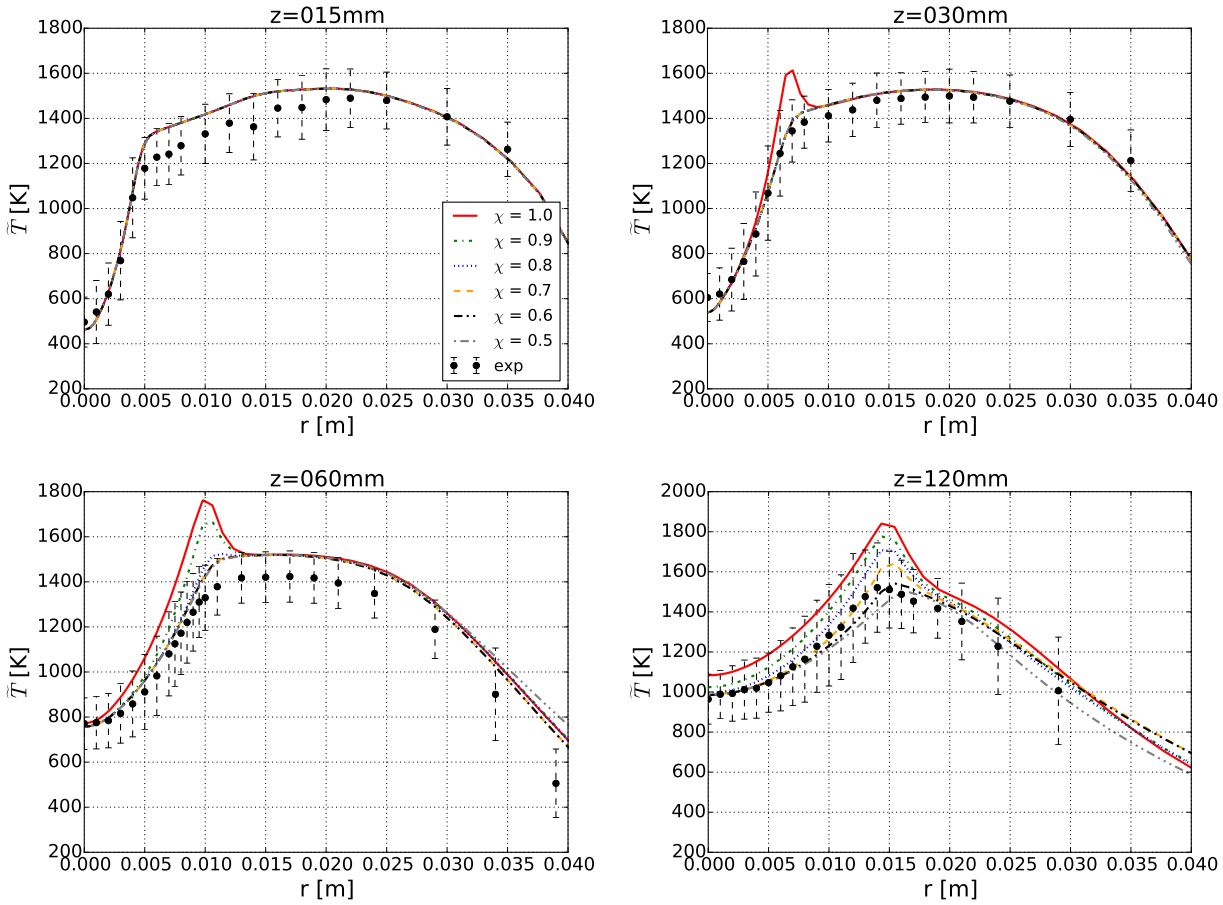

Figure 5: The temperature distribution for the flame DJHC-I-S $Re = 4100$ for the axial positions; 15 mm, 30 mm, 60 mm and 120 mm downstream of the nozzle. The results present the effect of gradual decrease in the value of reacting fraction of the fine structures χ.

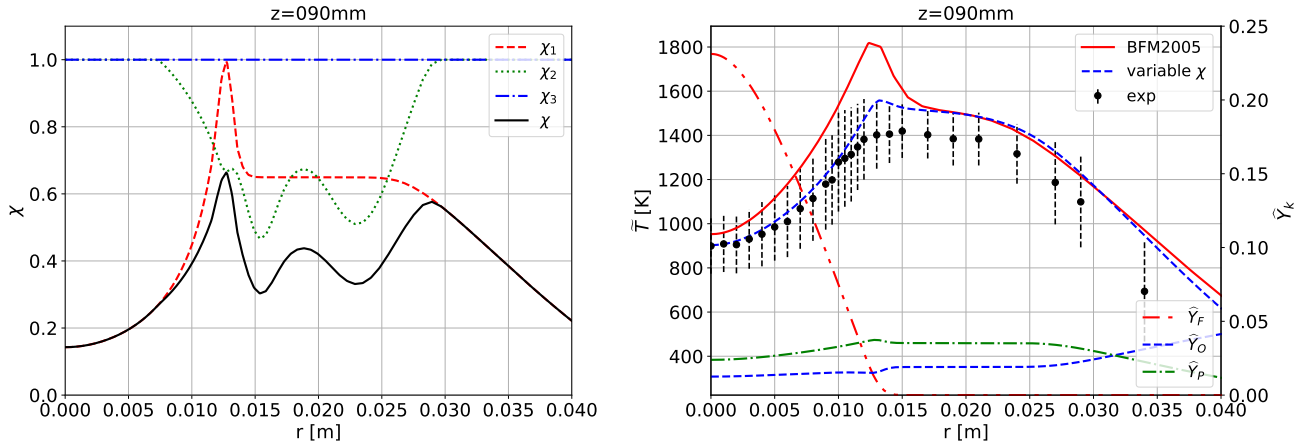

Figure 6: The radial distribution of the reacting fraction χ at the location z = 90 mm for the flame DJHC-I-S at Re=4100 on the finer grid M2 (left) and the radial distribution of temperature for the formulation of Magnussen [14] with $\chi = 1$ and with the variable value of χ (right). Right axis on right plots concerns distribution of $\widehat{Y}_\mathrm{F}$, $\widehat{Y}_\mathrm{O}$ and $\widehat{Y}_\mathrm{P}$.

standard set of constants giving $C_\gamma = 2.1377$, $C_\tau = 0.4082$ and $\gamma_\lambda < 1$ with $\chi = 1$. Simulations with any of the above parameters changed are denoted by a relevant caption in the legend of Figs. 7 - 10.

From the analysis presented in Section 5.1, it is interesting to note that clipping too high values of γ_λ had a strong effect on the decrease of reaction rate. It can be compared to the approach of changing C_γ, as in both cases the actual value of γ_λ is decreased. A lower value of C_γ leads to lower values of γ_λ everywhere in the domain, whereas clipping γ_λ at some point, corresponding to the certain turbulence Reynolds number, allows calculating the reaction rate as if the flow was more turbulent than it really is. Both methods prevent using too high values of γ_λ, yet the clipping seems to be more general as it affects the model only when approaching low turbulence Reynolds number. Thus, the method of clipping γ_λ can be presented as an alternative to the simulations with modified C_γ constant. These approaches were set together with the variable reacting fraction χ of the fine structures (cf. Section 5.2).

Both a decrease in χ and in C_γ reduce the reaction rate, hence lead to lower temperatures. It is noticeable that only the results obtained with the variable χ provided no peak temperature at the radial location z=30 mm and z=60 mm. For the case of Re=4100 at the location z=120 mm, the variable χ provided very good agreement with the experiment. However, for the higher Reynolds number case some temperature over-estimation was still observed downstream the flame. Nevertheless, all selected approaches led to more or less decrease in the temperature, and the effects of the discussed modifications were visible and consistent in both flames. This can be observed in Fig. 7, where radial temperature distributions are presented in the locations of 30, 60 and 120 mm downstream the nozzle for the two flow conditions. The biggest departures of simulation results from the experiments were observed for the radial distribution at the location 120 mm in the case of Re=8800. At that location, simulations with $C_\gamma = 1.0$ and variable χ again provided the best agreement with the experiment, yet with the maximum value higher by over 200 K. However, it was observed that when using $C_\gamma = 1.0$, the OH concentration downstream the flame was lower than upstream the jet. It can also be observed that the effect of C_γ and γ_λ correction was comparable in the locations closer to the nozzle. Further downstream, temperature results with modified C_γ were closer to those of the variable χ. Distributions of major species mass fraction are presented in Fig. 8, although the experimental data are not available. The relative comparison between the different modeling cases can be made, and for the major species conclusions can be drawn similar to those of the analysis of the temperature results. With the use of variable χ significant decrease of OH peak was observed, which comparing to the Adelaide JHC flames simulations [20, 67] is a correct trend.

Additionally, the lift-off occurrence was investigated with the OH radical mass fraction as an indicator of the ignition region. Figure 9 shows contours of OH mass fraction for five approaches applied on the two flames. The lift-off heights presented in Fig. 10 were determined as the axial distances form the nozzle where the mass fraction of OH increased over 2.8×10^{-4} [30]. The trend of decrease in lift-off height with increased jet Reynolds number discussed by Oldenhof et al. [7] and De et al. [27], was observed in all the variants for the medium and high Reynolds number cases. The formulation of Magnussen [14] with $\chi = 1$ highly under-predicted the lift-off height, and the modification in C_γ or clipping of γ_λ did not influence this effect as strongly as they did in case of reduction of temperature. Better predictions were obtained with changed values of reacting fraction of the fine structures, χ. However, it should be noted that proper relations between the lift-off height in the two flames were obtained when the value of χ was lower in case of the lower jet Reynolds number. When the contours of OH mean mass fraction were compared to the RMS values of the OH-fluorescence signal in the flame stabilization region (Fig. 7 in Oldenhof et al. [7]), the best agreements were obtained in the cases where $\chi = 0.6$ for the flame DJHC-I at $Re = 2500$, $\chi = 0.8$ for the flame DJHC-I at $Re = 4100$ and $\chi = 0.9$ for the flame DJHC-I at $Re = 8800$. Also the differences between the three lift-off heights were predicted correctly only in these cases. This indicated dependency of χ on Re_τ (through γ_λ). On the other hand, it can be seen in Figs. 5 and 7 that the above values of χ did not sufficiently decrease the temperature values. This problem might be solved with proper capture of the radiation effects or, additionally, with the modified or limited value of γ_λ for low Reynolds number flows and accounting for the oxygen dilution. In this context the use of variable χ seems to be the most optimal choice, as it provided the best temperature results and relatively good predictions of lift-off heights at

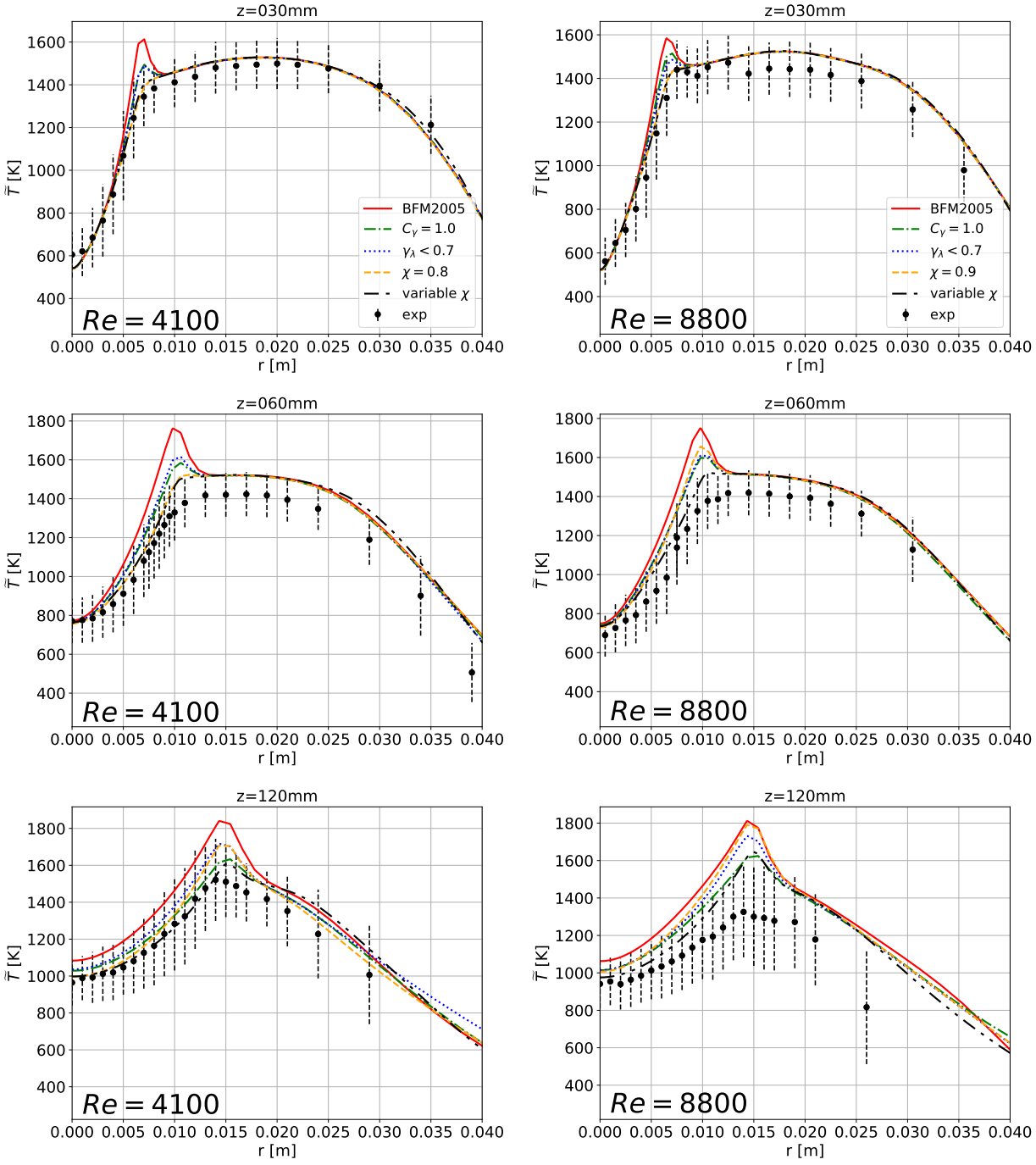

Figure 7: The radial temperature distribution for the flame DJHC-I-S Re = 4100 (left) and DJHC-I-S Re = 8800 (right) obtained with edcPisoFoam, with the five approaches of EDC at the axial positions; 30 mm, 60 mm and 120 mm downstream of the nozzle.

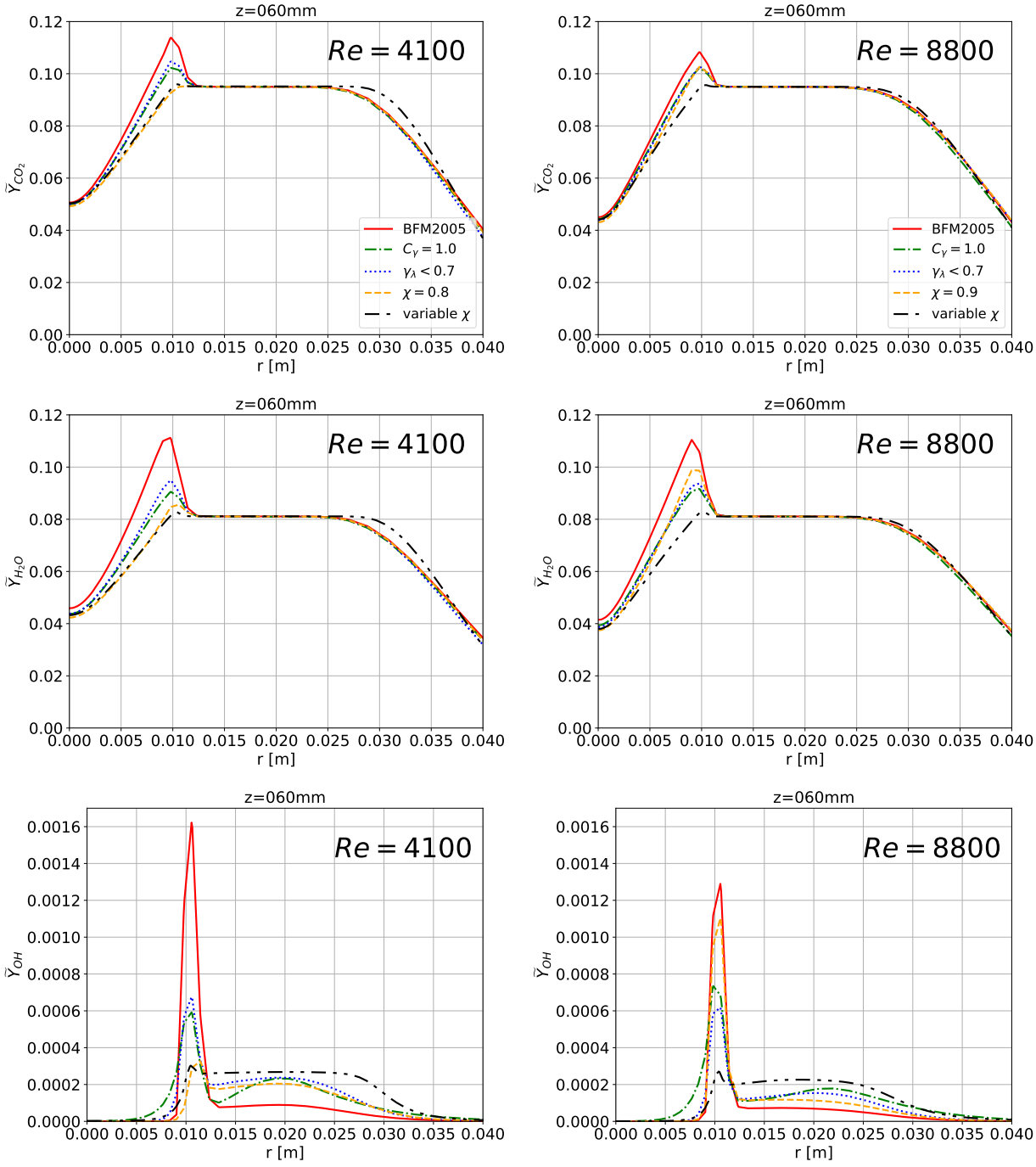

Figure 8: The radial CO_2, H_2O and OH distribution for the flame DJHC-I-S $Re = 4100$ (left) and DJHC-I-S $Re = 8800$ (right) obtained with edcPisoFoam, with the five approaches of EDC at the axial position z = 60 mm. No experimental data available.

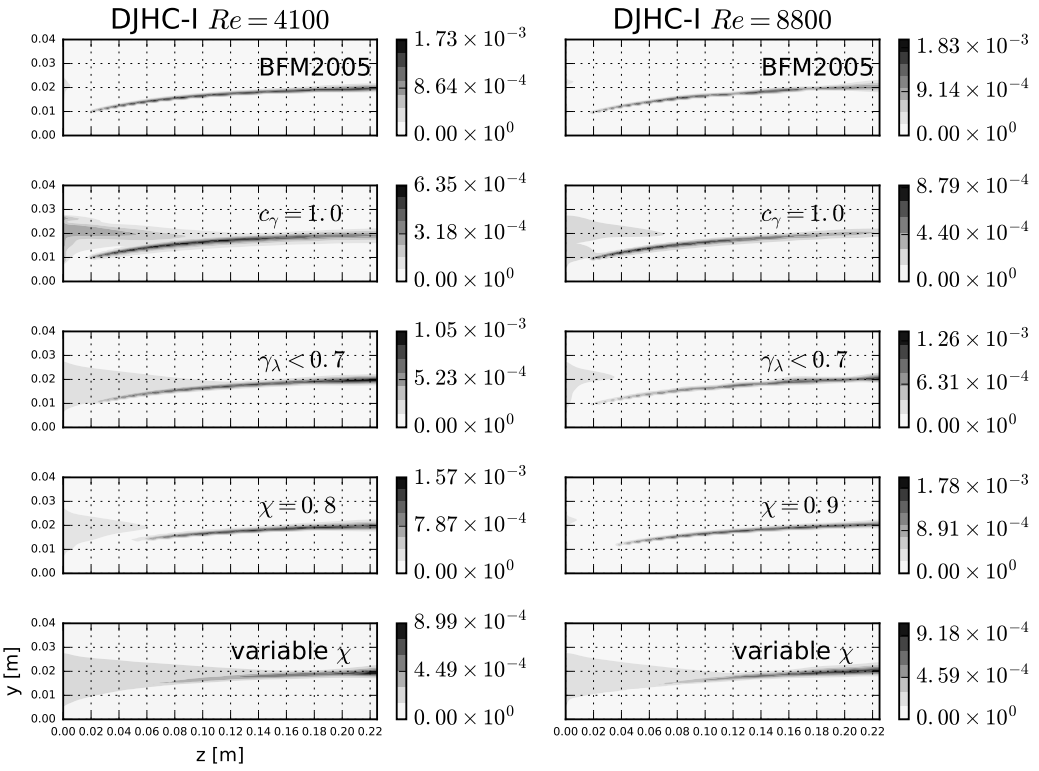

Figure 9: Contours of mass fraction of OH radicals for the flame DJHC-I-S $Re = 4100$ (left) and $Re = 8800$ (right) with the five approaches: the formulation of Magnussen [14] with $\chi = 1$, with changed C_γ constant, clipped value of γ_λ and with set value of reacting fraction χ. Note that the scale is different for every contour map.

the same time. However, the exact values of lift-off height were captured correctly for the case with medium Reynolds number, slightly overestimated for the high Reynolds number and it was underestimated for the low Reynolds number.

6. Conclusions

We have presented and discussed several factors that influence calculation of the reaction rate by the Eddy Dissipation Concept in the context of MILD combustion regime. The conditions of moderately low turbulence Reynolds number seem to play a crucial role for the reported temperature over-prediction by the EDC model. Considering the Perfectly Stirred Reactor model for the description of the fine structures in the detailed chemistry approach, the distinction between the surrounding and mean value of the mass fraction as the inflow condition to the reactor is meaningful. When the mean instead of surrounding value (as implemented, e.g., by Ansys Fluent) is used, the reaction rate increases with decreasing of turbulence Reynolds number. Moreover, the use of the mean value as the inflow value causes a difference in predictions by the formulations of Magnussen [14] and of Gran and Magnussen [13], so that the former gives a slightly higher reaction rate.

The strongly modified values of the secondary constants found in literature were considered and discussed in the context of the experiments they were originally derived for. Indeed, modification of the constants improves the predictions but has certain shortcomings. We have pointed out, that strongly modified EDC constants may lead to inconsistency with the turbulence models that are used. The discussion in Section 2.5 also showed that several groups of researchers proposed different adjusted set of EDC constants, which were sometimes contradictory to each other. This observation is rather persuading that there is no optimal set of EDC constants for MILD combustion in general.

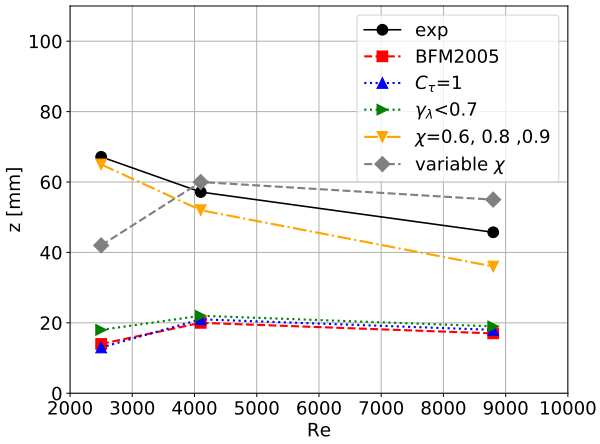

Figure 10: Lift-off heights position estimated based on OH radicals as a reaction zone indicator for the flames at three jet Reynolds number conditions. Symbols (•) represent experimental values of first occurrence of RMS of the OH-fluorescence signal in the flame stabilization region from [7]. Other symbols represent respective values obtained based on the mean mass fractions for the five different simulations.

This means that any EDC modifications aiming at extending its applicability to the MILD regime should capture the effects of low turbulence Reynolds number and slow chemistry by some functional expressions.

Low turbulence Reynolds number may require modification to the modeled fraction of the fine-structures regions, γ_λ. The simplest alternative is to introduce clipping at a certain value. The effect of change in the value of the secondary constant C_γ can be compared to clipping of the γ_λ. Changing the constant affects the whole spectrum of Re_τ, whereas clipping affects only the flow at the very low values of Re_τ. In this way the effect of reaction rate over-estimation is suppressed in the case of low turbulence Reynolds numbers, and the model is unchanged in other conditions with higher turbulence. Thus, in this approach, generality is preserved.

In most (or all) studies where modifications to the EDC constants are suggested, the fraction of reacting fine structures χ is set to unity. In the original EDC, this fraction is less than unity for low turbulence Reynolds numbers, for non-stoichiometric mixtures and for incomplete reactions. All these features apply locally to MILD combustion. As presented, a convenient approach to overcome the problem of too high reaction rate is the use of variable reacting fraction of the fine structures, χ as formulated in the original EDC by Magnussen. This is reasonable in MILD combustion, where the reaction zone is much broader and the fine structures occupy a large part of the space, and chemical pathways are affected by a coflow stream composition. We have presented the sensitivity of the EDC on this parameter and its effect on the temperature distribution and the prediction of lift-off height.

As all the proposed solutions decrease the temperature effectively, only the modified values of χ properly represent behavior of the lift-off in the context of the three flow conditions. We have presented that the approach of globally changed values and dynamically calculated local values of χ correctly reproduced experimental trends. The presented features of EDC revealed new approaches how to deal with over-predicted reaction rates by this model in MILD combustion regime.

7. Acknowledgments

We thank Professor Jacek Pozorski at IFFM Gdańsk for extensive discussions and comments on this paper. We are indebted to Professor Dirk Roekaerts at TU Delft for his courtesy to provide the experimental data of DJHC flames. We also thank Dr. Dmitry Lysenko for his courtesy to access the edcPisoFoam code. Calculations were carried out at the Academic Computer Centre in Gdańsk.

References

[1] J. A. Wunning, J. G. Wunning, Prog. Energy Combust. Sci. 23 (1997) 81–94.

[2] I. M. Katsuki, T. Hasegawa, Proc. Combust. Inst. 27 (1998) 3135–3146.

[3] D. R. Hardesty, F. J. Weinberg, Combust. Sci. Technol. 8 (1973) 201–2015.

[4] A. Cavaliere, M. de Joannon, Prog. Energy Combust. Sci. 30 (2004) 329–366.

[5] R. Weber, J. P. Smart, W. vd Kamp, Proc. Combust. Inst. 30 (2005) 2623–2629.

[6] M. Mancini, P. Schwoppe, R. Weber, S. Orsino, Combust. Flame 150 (2007) 54–59.

[7] E. Oldenhof, M. J. Tummers, E. H. van Veen, D. J. E. M. Roekaerts, Combust. Flame 158 (2011) 1553–1563.

[8] B. B. Dally, A. N. Karpetis, R. S. Barlow, Proc. Combust. Inst. 29 (2002) 1147–1154.

[9] K. Kwiatkowski, E. Mastorakos, Energ. Fuel. 30 (2016) 4386–4397.

[10] M. de Joannon, G. Sorrentino, A. Cavaliere, Combust. Flame 159 (2012) 1832–1839.

[11] B. F. Magnussen, in: 19th. AIAA aerospace science meeting, St. Louis, Missouri.

[12] B. F. Magnussen, in: 1st Topic Oriented Technical Meeting, Int. Flame Research Fundation, Amsterdam, Holland, 1989.

[13] I. R. Gran, B. F. Magnussen, Combust. Sci. Technol. 119 (1996) 191–217.

[14] B. F. Magnussen, in: ECCOMAS Thematic Conference on Computational Combustion, Lisbon, Portugal.

[15] I. S. Ertesvåg, B. F. Magnussen, Combust. Sci. Technol. 159 (2000) 213–235.

[16] D. Veynante, L. Vervisch, Prog. Energy Combust. Sci. 28 (2002) 193–266.

[17] Y. Minamoto, N. Swaminathan, S. R. Cant, T. Leung, Combust. Flame 161 (2014) 2801–2814.

[18] F. C. Christo, B. B. Dally, Combust. Flame 142 (2005) 17–129.

[19] A. Parente, J. C. Sutherland, B. B. Dally, L. Tognotti, P. J. Smith, Proc. Combust. Inst. 33 (2011) 3333–3341.

[20] A. Parente, M. Malik, F. Cantino, A. Cuoci, B. B. Dally, Fuel 163 (2016) 98–111.

[21] A. Rebola, P. J. Coelho, M. Costa, Combust. Sci. Technol. 185 (2013) 600–626.

[22] M. Ihme, J. Zhang, G. He, B. Dally, Flow Turbul. Combust. 89 (2012) 449–464.

[23] C. Locci, O. Colin, J. B. Michel, Flow Turbul. Combust. 93 (2014) 305–347.

[24] O. Colin, J. B. Michel, Flow Turbul. Combust. 97 (2016) 631–662.

[25] A. S. Verissimo, A. M. A. Rocha, M. Costa, Energ. Fuel. 25 (2011) 2469–2480.

[26] M. U. Goktolga, J. A. van Oijen, L. P. H. de Goey, Proc. Combust. Inst. 36 (2017) 4269–4277.

[27] A. De, E. Oldenhof, P. Sathiah, D. J. E. M. Roekaerts, Flow Turbul. Combust. 87 (2011) 537–567.

[28] M. J. Evans, P. R. Medwell, Z. F. Tian, Combust. Sci. Technol. 187 (2015) 1093–1109.

[29] S. H. Kim, K. Y. Huh, B. B. Dally, Proc. Combust. Inst. 30 (2005) 751–157.

[30] A. Tyliszczak, Arch. Mech. 65 (2013) 97–129.

[31] J. W. Labahn, D. Dovizio, C. B. Devaud, Proc. Combust. Inst. 35 (2015) 3547–3555.

[32] J. W. Labahn, C. B. Devaud, Combust. Flame 164 (2016) 68–84.

[33] B. Danon, W. de Jong, D. J. E. M. Roekaerts, Combust. Sci. Technol. 182 (2010) 1261–1278.

[34] Z. Mao, L. Zhang, X. Zhu, D. Zhou, W. Liu, C. Zheng, Appl. Therm. Eng. 111 (2017) 387–396.

[35] M. Vascellari, G. Cau, Fuel 101 (2012) 90–101.

[36] M. Vascellari, S. Schulze, P. Nikrityuk, D. Safronov, C. Hasse, Flow Turbul. Combust. 92 (2014) 319–345.

[37] B. Liu, Y. H. Wang, H. Xu, Appl. Therm. Eng. 91 (2015) 1048–1058.

[38] D. Lupant, P. Lybaer, Appl. Therm. Eng. 75 (2015) 93–102.

[39] V. Fortunato, C. Galletti, L. Tognotti, A. Parente, Appl. Therm. Eng. 76 (2015) 324–334.

[40] B. Danon, E.-S. Cho, W. de Jong, D. J. E. M. Roekaerts, Appl. Therm. Eng. 31 (2011) 3885–3896.

[41] A. Parente, C. Galletti, L. Tognotti, Int. J. Hydrogen Energy 33 (2008) 7553–7564.

[42] M. Graca, A. Duarte, P. J. Coelho, M. Costa, Fuel Process. Technol. 107 (2013) 126–137.

[43] J. Aminian, C. Galletti, S. Shahhosseini, L. Tognotti, Flow Turbul. Combust. 88 (2012) 597–623.

[44] M. Rehm, P. Seifert, B. Meyer, Comput. Chem. Eng. 33 (2009) 402–407.

[45] S. R. Shabanian, P. R. Medwell, M. Rahimi, A. Frassoldati, A. Cuoci, Appl. Therm. Eng. 52 (2013) 538–554.

[46] Y. Tu, K. Su, H. Liu, S. Chen, Z. Liu, C. Zheng, Energ. Fuel. 30 (2016) 1390–1399.

[47] J. Aminian, C. Galletti, L. Tognotti, Fuel 165 (2016) 123–133.

[48] B. Lilleberg, D. Christ, I. S. Ertesvåg, K. E. Rian, R. Kneer, Flow Turbul. Combust. 91 (2013) 319–346.

[49] A. Shiehnejadhesar, R. Mehrabian, R. Scharler, G. M. Goldin, I. Obernberger, Fuel 126 (2014) 177–187.

[50] A. Mardani, Fuel 191 (2017) 114–129.

[51] T. Myhrvold, I. S. Ertesvåg, I. R. Gran, R. Cabra, J.-Y. Chen, Combust. Sci. Technol. 178 (2006) 1001–1030.

[52] H. G. Weller, G. Tabor, H. Jasak, C. Fureby, Comput. Phys. 12 (1998) 620–631.

[53] D. A. Lysenko, I. S. Ertesvåg, K. E. Rian, Flow Turbul. Combust. 93 (2014) 577–605.

[54] D. A. Lysenko, I. S. Ertesvåg, K. E. Rian, Flow Turbul. Combust. 93 (2014) 665–687.

[55] Ansys Fluent Theory Guide, 2013. Release 15.0.

[56] A. Cuoci, M. R. Malik, A. Parente, in: 23rd Journes dEtude of the Belgian Section of the Combustion Institute, Brussels, Belgium.

[57] B. E. Launder, D. B. Spalding, Comput. Method. Appl. M. 3 (1974) 269–289.

[58] H. Tennekes, Phys. Fluids 11 (1968) 669–671.

[59] J. P. Jessee, R. F. Gansman, W. A. Fiveland, Heat Transfer in Fire and Combustion System (ASMEed.) 250 (1993) 43–53.

[60] Z. Li, A. Cuoci, A. Sadiki, A. Parente, Energy 139 (2017) 555–570.

[61] T. Myhrvold, Combustion modeling in turbulent boundary-layer flows, Dr. ing. thesis 2003:38, NTNU Norwegian University of Science and Technology, Trondheim, Norway, 2003.

[62] I. S. Ertesvåg, Development of a turbulence model for low Reynolds numbers with an equation for the Reynolds stresses and an equation for a characteristic frequency (in Norwegian), Dr. ing. thesis 1991:49, Department of Thermodynamics, Norwegian Institute of Technology, Trondheim, Norway, 1991.

[63] P. G. Saffman, D. C. Wilcox, AIAA J. 12 (1974) 541–546.

[64] D. C. Wilcox, AIAA J 26 (1988) 1299–1310.

[65] V. Yakhot, S. A. Orszag, S. Thangam, T. B. Gatski, C. G. Speziale, Phys. Fluids A-Fluid 4 (1992) 1510–1520.

[66] I. S. Ertesvåg, Turbulent Flow and Combustion (in Norwegian), Tapir Academic Publisher, Trondheim, Norway, 2000.

[67] A. Frassoldati, P. Sharma, A. Cuoci, T. Faravelli, E. Ranzi, Appl. Therm. Eng. 30 (2010) 376–382.

[68] M. T. Lewandowski, P. Pluszka, J. Pozorski, Int. J. Num. Meth. Heat Fluid Flow (2017) DOI:10.1108/HFF–02–2017–0078. (in press).

[69] M. J. Evans, P. R. Medwell, H. Wu, A. Stagni, M. Ihme, Proc. Combust. Inst. 36 (2017) 4297–4304.

[70] M. J. Evans, P. R. Medwell, Z. F. Tian, J. Ye, A. Frassoldati, A. Cuoci, Combust. Flame 178 (2017) 297–310.

[71] J. A. M. Sidey, E. Mastorakos, Combust. Flame 163 (2016) 1–11.

[72] S. B. Pope, Combust. Theor. Model 1 (1997) 41–63.

[73] J. J. McGuirk, W. Rodi, in: B. Launder, F. Schmidt, J. Whitelaw (Eds.), 1st Symp. on Turbulent Shear Flows, Springer-Verlag, Berlin Heidelberg, Germany, 1979, pp. 71–83.

[74] T. H. Shih, W. W. Liou, A. Shabbir, Z. Yang, J. Zhu, Computers Fluids. 24 (1995) 227–238.

[75] B. E. Launder, B. I. Sharma, Lett. Heat Mass Trans. 1 (1974) 131–138.

[76] S. B. Pope, AIAA J. 16 (1978) 279–281.

[77] B. B. Dally, D. F. Fletcher, A. R. Masri, Combust. Theor. Model. 2 (1998) 193–219.

[78] C. M. Or, K. M. Lam, P. Liu, J. of Hydro-environ. Res. 5 (2011) 81–91.

[79] G. J. Nathan, J. Mi, Z. T. Alwahabi, G. J. R. Newbold, D. S. Nobes, Prog. Energy Combust. Sci. 32 (2007) 496–538.

[80] E. H. Chui, G. D. Raithby, Numer. Heat Transfer B 23 (1993) 269–288.

[81] A. Kazakov, M. Frenklach, Reduced reaction set based on GRI-Mech 1.2: DRM19, http://www.me.berkeley.edu/drm, Accessed: 2015-08-15.

[82] P. Sabia, M. de Joannon, A. Picarelli, A. Chinnici, R. Ragucci, Fuel 91 (2012) 238–245.

[83] M. L. Lavadera, P. Sabia, G. Sorrentino, R. Ragucci, M. de Joannon, Fuel 184 (2016) 876–888.

[84] Y. Tu, W. Yang, H. Liu, Energ. Fuel. 31 (2017) 10144–10157.

[85] A. De, A. Dongre, Flow Turbul. Combust. 94 (2015) 439–478.

[86] C. M. Rhie, W. L. Chow, AIAA J. 21 (1983) 1525–1532.

[87] E. Hairer, G. Wanner, Solving ordinary differential equations II: Stiff and differential-algebraic problems, Springer Series in Computational Mathematics, 2nd ed., Springer-Verlag, Berlin Heidelberg, Germany, 1996.